



Particle flux on the continental shelf in the Amundsen Sea Polynya and Western Antarctic Peninsula

Hugh W. Ducklow^{1*} • Stephanie E. Wilson² • Anton F. Post³ • Sharon E. Stammerjohn⁴ • Matthew Erickson⁵ • SangHoon Lee⁶ • Kate E. Lowry⁷ • Robert M. Sherrell⁸ • Patricia L. Yager⁹

¹Lamont-Doherty Earth Observatory, Columbia University, Palisades, New York, United States

²Bangor University, Bangor, Gwynedd, United Kingdom

³University of Rhode Island, Narragansett, Rhode Island, United States

⁴University of Colorado, Boulder, Colorado, United States

⁵Antarctic Support Contractor, Arlington, Virginia, United States

⁶Korean Polar Research Institute, Seoul, Korea

⁷Stanford University, Palo Alto, California, United States

⁸Rutgers University, New Brunswick, New Jersey, United States

⁹University of Georgia, Athens, Georgia, United States

*hducklow@ldeo.columbia.edu

Abstract

We report results from a yearlong, moored sediment trap in the Amundsen Sea Polynya (ASP), the first such time series in this remote and productive ecosystem. Results are compared to a long-term (1992–2013) time series from the western Antarctic Peninsula (WAP). The ASP trap was deployed from December 2010 to December 2011 at 350 m depth. We observed two brief, but high flux events, peaking at 8 and 5 mmol C m⁻² d⁻¹ in January and December 2011, respectively, with a total annual capture of 315 mmol C m⁻². Both peak fluxes and annual capture exceeded the comparable WAP observations. Like the overlying phytoplankton bloom observed during the cruise in the ASP (December 2010 to January 2011), particle flux was dominated by *Phaeocystis antarctica*, which produced phytodetrital aggregates. Particles at the start of the bloom were highly depleted in ¹³C, indicating their origin in the cold, CO₂-rich winter waters exposed by retreating sea ice. As the bloom progressed, microscope visualization and stable isotopic composition provided evidence for an increasing contribution by zooplankton fecal material. Incubation experiments and zooplankton observations suggested that fecal pellet production likely contributed 10–40% of the total flux during the first flux event, and could be very high during episodic krill swarms. Independent estimates of export from the surface (100 m) were about 5–10 times that captured in the trap at 350 m. Estimated bacterial respiration was sufficient to account for much of the decline in the flux between 50 and 350 m, whereas zooplankton respiration was much lower. The ASP system appears to export only a small fraction of its production deeper than 350 m within the polynya region. The export efficiency was comparable to other polar regions where phytoplankton blooms were not dominated by diatoms.

Introduction

Export of organic matter is an important biogeochemical process contributing to the carbon balance in terrestrial and marine ecosystems (Chapin III et al., 2005), and is the key carbon exchange between biomes in the earth system. In the ocean, export is defined as the transport, by sinking, advection or migration, of dissolved and particulate organic carbon (DOC and POC) from the productive surface layer (euphotic zone or upper ca. 50–100 m of the open sea) to the ocean interior (Ducklow, 1995; Henson et al., 2012). Net community production (NCP, gross primary production minus community respiration) sets an upper limit to

Domain Editor-in-Chief

Jody W. Deming, University of Washington

Knowledge Domain

Ocean Science

Article Type

Research Article

Part of an *Elementa* Special Feature

ASPIRE: The Amundsen Sea Polynya International Research Expedition

Received: July 7, 2014

Accepted: March 22, 2015

Published: April 17, 2015

the amount of organic matter available for export in marine pelagic systems remote from land or not subject to lateral inputs of organic matter (Ducklow and Doney, 2013). Particle export can be estimated from short-term (days) drifting sediment traps or moored traps deployed over longer (annual) periods, and from Uranium-238 to Thorium-234 disequilibria in the upper water column (Buesseler, 1991; Honjo et al., 2008; Henson et al., 2012). Dissolved organic matter may comprise 15–20% of the total NCP or export globally (Carlson et al., 1994; Hansell and Carlson, 1998). Sediment traps do not capture the dissolved component of the export flux.

The magnitude of the particulate export flux varies within and between ocean regions as a function of primary productivity and temperature (Laws et al., 2000) and also interannually (Ducklow et al., 2008; Church et al., 2013). Export fluxes from the upper 100 m, as estimated from sediment trap collections, ranged from 1 to 10 mmol C m⁻² d⁻¹ across three open ocean provinces (Central Equatorial Pacific, Arabian Sea, Southern Ocean) and reached 25 mmol C m⁻² d⁻¹ in the North Atlantic (Berelson, 2001). Henson et al. (2012) reported a wider range of export fluxes, from near zero to over 40 mmol C m⁻² d⁻¹, using a global compilation of export values derived from Thorium disequilibria. Normalizing the export flux to the corresponding primary productivity yields the export efficiency, a useful metric for comparing ocean ecosystem carbon fluxes (Buesseler, 1998). Particle export efficiency ranges from near zero to around 50% (and with outliers exceeding 100%). There is a tendency for export efficiency to be greater in polar seas (Henson et al. 2012), as might be expected from the physiological effects of temperature on consumption processes (López-Urrutia et al., 2006).

Much of the export is decomposed and remineralized in the mesopelagic ocean between the base of the euphotic zone and ca. 1000 m, the ‘Twilight Zone’ (Martin et al., 1987; Buesseler et al., 2007b; Giering et al., 2014). Many studies report that the export flux leaving ca. 100 m is greatly attenuated by the time it is captured in sediment traps moored or deployed in the twilight zone. A greater fraction of the export is typically remineralized at more shallow depths in warmer water (Marsay et al. 2015). Together the processes of export and its consumption in the upper 1000 m determine the amount of carbon ultimately stored in the deep ocean, isolated from exchange with the atmosphere over time scales of centuries to millennia. The processes governing the export and the efficiency of its transfer to the deep sea are poorly understood, especially in the Southern Ocean, an important ocean CO₂ sink (Takahashi et al., 2009); and also in the Arctic Ocean, a region of pronounced climate and ecosystem change (Tremblay et al., 2012). Here we focus on the Amundsen Sea, Antarctica.

The seasonal sea ice zone (SIZ) of Antarctica, generally extending 500–1500 km from the coast across the continental shelf and bounded by the Antarctic Circumpolar Current at its equatorward extent, is a region of high primary and secondary productivity during the summer ice-free period. Prolonged darkness and heavy ice cover in winter severely limit biological processes dependent on recent, local primary production. The extreme seasonality of the SIZ offers a powerful tool for studying physical and biological controls on export processes. There have been numerous studies of particle flux in both polar seas using sediment traps (Fischer et al., 1988; Collier et al., 2000; Anadon and Estrada, 2002; Fischer et al., 2002; Ducklow et al., 2008; Sampei et al., 2011, 2012; Honjo et al., 2010; Forest et al., 2011; Weston et al., 2013) and Thorium-234/Uranium-238 disequilibria (Cochran et al., 2000; Amiel et al., 2002, 2008; Buesseler et al., 2010). These reports all show that particle flux tends to be dominated by a relatively brief annual high flux event (a “peak”), following the spring-summer phytoplankton blooms typical of the SIZ environment. Both very low (~ 10–100 μmol C m⁻² d⁻¹; Honjo et al., 2010, in the Arctic) and very high fluxes (5–10 mmol C m⁻² d⁻¹; Collier et al., 2000, Ross Sea, Antarctica, and this paper) have been observed by sediment traps in polar seas.

Polynyas, ice-free areas surrounded by variable, seasonal or persistent sea ice cover, are zones of locally enhanced primary (Smith Jr and Gordon, 1997; Arrigo and van Dijken, 2003) and secondary productivity (Ducklow and Yager, 2007). Until now, intensive biogeochemical studies in Antarctic polynyas have only been performed in the Ross Sea Polynya (RSP, Smith Jr et al., 2000), including sediment trap deployments (Collier et al., 2000). The Amundsen Sea Polynya (ASP) is the most productive of the Antarctic polynyas, and possibly the most productive marine ecosystem in Antarctica (Arrigo et al., 2012). The Amundsen Sea International Research Expedition (ASPIRE; Yager et al., 2012) afforded us the opportunity to deploy a moored sediment trap over a yearlong period in this rarely visited region, in conjunction with a range of other physical, biogeochemical and ecological observations (this Special Feature). The RVIB Araon cruise (Korean Polar Research Institute), immediately following the ASPIRE cruise, complemented our research with a yearlong sediment trap deployment below the heavier sea ice cover northwest of the ASP, about 250 km from our mooring (Kim et al., 2014). These yearlong sediment trap deployments provide the only extended *in situ* data on biogeochemical processes in the polynya interior. Enhanced seasonality and high production in polynyas, especially in the ASP, constitute a valuable case study for relating the particle flux at depth to the overlying production of exportable organic matter and its seasonality. In this paper we present the sediment trap results and compare the derived fluxes to an analysis of key processes in the ASP carbon cycle synthesized from ASPIRE investigations (Mu et al., 2014; Williams et al., 2015; Wilson et al., 2015).

A key challenge confronting biogeochemical research in Antarctica is the pronounced interannual variability typical of the Southern Ocean and Antarctic SIZ. For example, most sediment trap deployments last just a single year or less, making it difficult to generalize about patterns and magnitudes of flux, especially its seasonality. The Palmer Antarctica Long Term Ecological Research project has deployed a moored time series

sediment trap on the continental shelf to the west of the Antarctic Peninsula (WAP) annually since 1992 (Ducklow et al., 2008). Results from this over twenty-year time series provide a long-term context in which to interpret the ASP observations. The Bellingshausen-Amundsen Sea region of West Antarctica and the WAP have been experiencing rapid atmospheric and ocean warming (Meredith and King, 2005) and pronounced declines in sea ice cover (Stammerjohn et al., 2012). The northern WAP, with about 100–150 days of ice cover annually, presents a notable contrast to the Amundsen Sea, with 212–274 days of ice cover annually (Arrigo et al., 2012). In this paper we present results from our sediment trap deployment in the ASP, and compare the fluxes to observations in the WAP during the same year and over the past two decades. With these results we: 1) interpret the seasonality of particle fluxes in the ASP, WAP and other Antarctic locations; 2) deduce the sources of the flux from biogeochemical measurements, zooplankton fecal pellet measurements and microscopic observations; 3) consider the relationship between fluxes recorded in sediment trap collections and the overlying production and export rates; and 4) identify unresolved issues requiring further study.

Materials and methods

Study region

The Amundsen Sea Polynya International Research Expedition (ASPIRE) was conducted in the Amundsen Sea Polynya (ASP, Figure 1) aboard the US Research Vessel Icebreaker (RVIB) *Nathaniel B Palmer* in December 2010 to January 2011 (Yager et al., 2012). Comprehensive oceanographic and ecological studies, including an annual sediment trap deployment, have been conducted by the Palmer Long Term Ecological Research project over the continental shelf to the west of the Antarctic Peninsula (WAP, Figure 1A, inset) since 1992 (Ducklow, 2008; Steinberg et al., 2012). The WAP sediment trap, chlorophyll, and sea ice observations from 2010–2012 are presented in this paper for comparison with the ASPIRE observations 1200 km farther south.

Sediment trap mooring: Amundsen Sea Polynya

We deployed a Technicap PPS 3/3 24S time series sediment trap (SARL Technicap, La Turbie, France, <http://www.technicap.com/products/traps/design.htm>). It is a cylindrical trap with an internal funnel below a baffled 0.125 m² opening and is equipped with 24 sample cups. This trap was designed to minimize hydrodynamic shear from the ambient current field around the trap that can interfere with particle collection

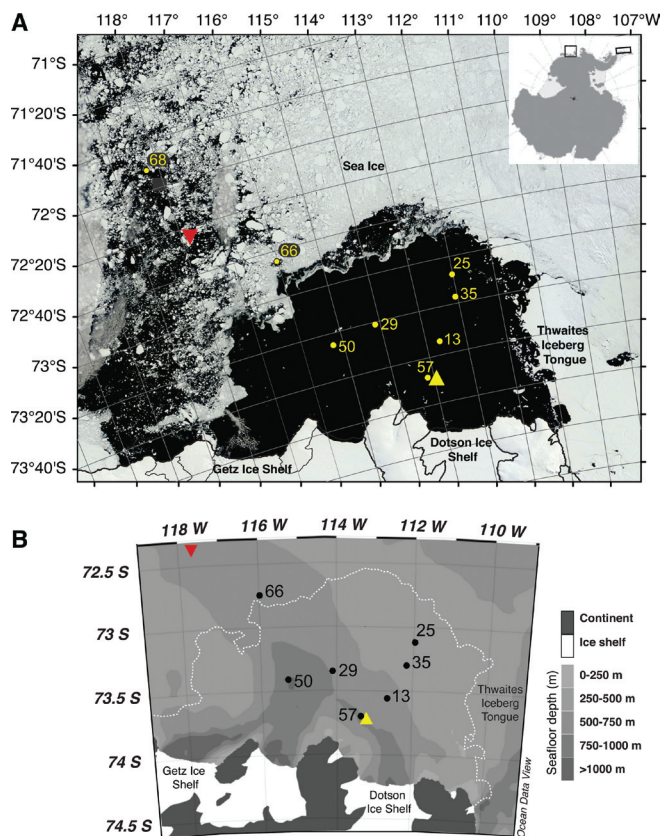


Figure 1

Maps of Amundsen Sea region.

Maps show the Amundsen Sea Polynya and locations of major ASPIRE hydrological stations and moored sediment traps. Yellow and red triangles indicate the ASPIRE and Korean trap locations, respectively. A Moderate Resolution Imaging Spectroradiometer (MODIS) Terra satellite image from 02 January 2011 shows the open water (polynya) area (A); regional bathymetry is shown in (B).

doi: 10.12952/journal.elementa.000046.f001

(see Discussion). The sediment trap mooring was equipped with dual Benthos 866A Acoustic Transponding Releases (Teledyne Benthos, North Falmouth, MA USA; http://www.benthos.com/index.php/product/acoustic_releases/866-a). The mooring was deployed from RVIB NB Palmer at 73° 49.254' South, 113° 04.033' West on 16 December 2010 in an area of the Amundsen Sea Polynya selected for its deep bottom depth, reliable open water conditions in December (from satellite SSM/I observations, see below), and remote ocean color imagery as being typical of the central, high productivity waters of the ice-free polynya region. The mooring was close to ASPIRE Station 57.02, which was visited 15 days after trap deployment (Figure 1). The mooring was configured with the trap at approximately 350 m below the surface in a water depth of 800 m. The trap was programmed to sample from 18 December 2010 to 04 January, 2012 at intervals of 7–14 days during expected spring–summer periods of high primary productivity (November–January) and 30–62 days in the winter. The mooring was recovered successfully by RVIB Araon on 16 February 2012.

Sediment trap mooring: Western Antarctic Peninsula

Sediment trap results from the Palmer Long Term Ecological Research (LTER) project on the western Antarctic Peninsula for 2010–2012 are included for comparison with the ASP results. A McLane Mark IV PARFLUX times series trap has been deployed annually at approximately 64° 30' South, 66° 04' West since 1993 (Ducklow et al., 2008). This trap has a large (0.5 m² aperture) collecting cone. It is moored at 170 m depth in a 350-m water column on the mid-continental shelf about 130 km west of Palmer Station.

Sediment trap sample analysis

Sample cups in the ASP and WAP traps were filled with buffered 2% formaldehyde in filtered seawater adjusted to 5% NaCl prior to deployment. Following their return to the USA, samples were analyzed following the JGOFS Protocols (Knap et al., 1996). We carefully removed all apparent zooplankton swimmers under a dissecting microscope prior to sample processing. Samples were split using a 10-place rotary wet sample divider (McLane Research Labs, North Falmouth, MA USA; http://www.mclanelabs.com/sites/default/files/sub_page_files/McLane-WSD-10-Datasheet.pdf). Sample splits were either combined or split again depending on the amounts of sediment in each cup. When sufficient material was available, half of the sample was retained and archived for reference and possible future analyses. Separate sample splits were filtered and analyzed for total dry mass and for particulate organic carbon and nitrogen content. Prior to analysis, samples were rinsed with distilled water to remove sea salt. We found no difference in the organic C and N content between samples rinsed with distilled water or filtered seawater. Prior to C and N determination, samples were rinsed with dilute HCl to remove carbonate, and then rinsed with distilled water.

Particulate organic carbon (POC), particulate nitrogen, and their isotopic composition (ASP only) were determined using a Europa ANCA-SL elemental analyzer interfaced with the Europa 20–20 CF-IRMS at The Ecosystems Center's Stable Isotope Lab (Marine Biological Lab, Woods Hole, MA USA; <http://www.mbl.edu/ecosystems/silab/>).

Sea ice and chlorophyll

Satellite measurements of sea-ice concentration are from the Defense Meteorological Satellite Program's (DMSP) Special Sensor Microwave/Imager (SSM/I). They were determined using the Bootstrap passive microwave algorithm, from which a time series was created that minimized differences between the various SSM/I sensors (Stammerjohn et al., 2008). This study uses the daily SSM/I time series (2010–2012) as provided by the EOS Distributed Active Archive Center (DAAC) at the National Snow and Ice Data Center, University of Colorado in Boulder, Colorado (<http://nsidc.org>). The sea-ice concentration data are for a 25 by 25 km area centered over the mooring site at each location considered in our comparative analysis. Sea ice advance and retreat are defined as the first and last day, respectively, that sea ice cover passes 15% concentration for five consecutive days (Stammerjohn et al., 2008). Sea ice year is defined based on the long-term average dates of advance and retreat for each region. The sea ice year for the ASP starts on 15 February and ends on 14 February of the following year. For the WAP region, the year extends from 15 to 14 March.

Estimates of Chlorophyll *a* concentration were retrieved from MODIS ocean color observations (Reprocessing R2009.1) using the OC3M algorithm (O'Reilly et al., 2000). All reported values were extracted from daily composite images of the ASP and WAP and averaged over a 31 km² grid over each sediment trap location.

Zooplankton contribution to particle flux

To determine fecal pellet production rates and their potential POC flux, zooplankton were collected live and in good condition using a 333 µm mesh ring net with a non-filtering cod-end bucket on 26 December (ASPIRE Station 35, Figure 1) and 05 January (ASPIRE Station 66). Upon collection, the dominant species *Euphausia crystallarophias*, *Calanoides acutus*, and *Metridia gerlachei* were selected, sorted by species, and gently rinsed in filtered seawater before being placed in 1-L incubation chambers with an interior collector that separates

fecal pellets from individuals to avoid coprophagy. The pellet collectors were modified Tricorn beakers with 500 or 1000 μm mesh glued to the bottom and placed in 1-L straight-sided jars. One-three *E. crystallarophias*, five *C. acutus* or five *M. gerlachei* were placed in separate, triplicate chambers for each species and incubated for 6–12 hours. After the incubation was terminated, the fecal pellets collected at the bottom of the jars were counted, photographed digitally, and preserved at -80°C for future molecular analyses. ImageJ Software was used to measure pellet length and width to calculate volumes of the fecal pellets based on the volumes of ovoid and cylinder shapes and converted into carbon values as measured in (Gleiber et al., 2012). We calculated potential POC fluxes for target species from these measurements and MOCNESS tows at ASPIRE sampling stations 13, 25, 35, 50 and 57 (Figure 1) for depth-integrated zooplankton abundance data to 150 m. Flux values from the sediment trap covering the period of zooplankton sampling were used for this comparison.

Other measurements and observations

A number of other quantities were used in our analysis of particle flux in the Amundsen Sea Polynya, as described briefly here. Details of the measurements and derivations are given in other papers in this Special Feature, as cited. Net primary production rates were measured by 24-hour shipboard incubations of seawater samples with ^{14}C -bicarbonate. Net community production and export, were derived from changes in nutrient and carbon inventories (Yager et al., 2014). Bacterial production and community respiration rates, measured using ^3H -leucine incorporation and CO_2 production during 24–48 hour dark incubations, were obtained from Williams et al. (2015).

ASP sediment trap data are available at the BCO-DMO website (BCO-DMO ASPIRE site, <http://www.bco-dmo.org/project/2132>). Palmer LTER data are available at: (<http://oceaninformatics.ucsd.edu/datazoo/data/pallter/datasets>; Dataset number 26, “Offshore sediment trap fluxes”). In the results and discussion below, we define the particulate carbon flux departing the upper 100 m as the export flux to discriminate it from that captured by sediment traps at 350 m, termed as the trap flux, when needed for clarity.

Results

Sea ice and chlorophyll

Remotely observed sea ice cover, ocean color, and *in situ* sediment trap results all reflected the highly seasonal nature of the polar environment. Sea ice retreated from the trap location in the ASP on 18 November 2010, after 247 days of ice cover. The subsequent open water period lasted 100 days until 26 February 2011 (Figure 2A).

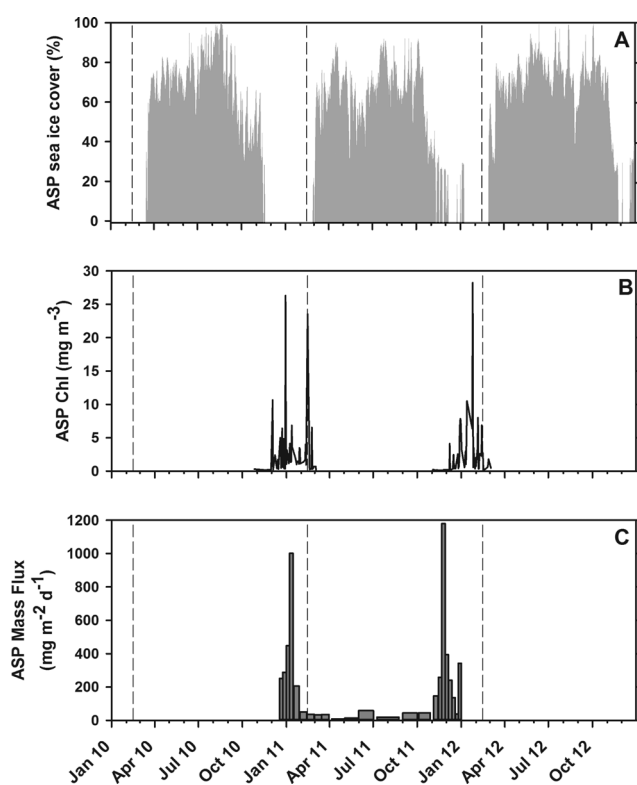
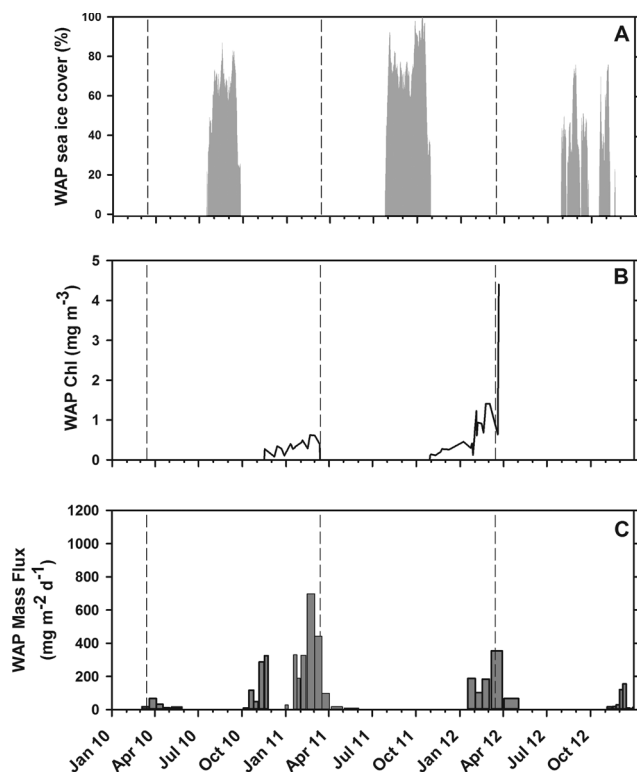


Figure 2
Sea ice cover and chlorophyll and particle flux in the ASP.

Percent sea ice cover (A), surface chlorophyll concentration (B), and vertical mass flux of sinking particulate matter (C) are shown for the sediment trap mooring site in the Amundsen Sea Polynya from January 2010 to December 2012. The dashed black lines mark the sea ice years 2010 (15 February 2010 to 14 February 2011) and 2011 (15 February 2011 to 14 February 2012). Width of flux bars in panel C indicates duration over which each sample cup in sediment trap was open and collecting (7–62 days, depending on season and expected flux).

doi: 10.12952/journal.elementa.000046.f002

**Figure 3**

Sea ice cover and chlorophyll and particle flux in the WAP.

Percent sea ice cover (A), surface chlorophyll concentration (B), and vertical mass flux of sinking particulate matter (C) are shown for the sediment trap mooring site in the western Antarctic Peninsula from January 2010 to December 2012. The dashed black lines mark the sea ice years 2010 (15 March 2010 to 14 March 2011) and 2011 (15 March 2011 to 14 March 2012). Width of flux bars in panel C indicates duration over which each sample cup in sediment trap was open and collecting (7–62 days, depending on season and expected flux). No visible bar indicates very low flux, not lack of sample.

doi: 10.12952/journal.elementa.000046.f003

In the 2011–2012 ice year, ice cover lasted 282 days, with ice retreat occurring somewhat later, on 6 December 2011. In contrast, sea ice cover at the WAP site (Figure 3A) lasted just 71 and 65 days in 2010 and 2011, respectively, with the open water period between lasting 303 days (26 September 2010 to 26 July 2011). In the two regions, percent ice cover was similar during the actual periods when sea ice covered the mooring region, averaging $65 \pm 20\%$ ($n=529$) for the two years in the ASP, and $67 \pm 19\%$ ($n=136$) in the LTER area.

In late 2010, surface chlorophyll in the ASP started to increase 1–2 weeks after the full ice retreat (15% threshold), indicating the initiation of the spring–summer phytoplankton bloom 15 days prior to our initial occupation of the ASP site (Figure 2B) and mooring installation. Chlorophyll (Chl) was relatively low ($\sim 5 \text{ mg m}^{-3}$) at the mooring site at the start of sediment trap collection, and reached its maximum surface concentration (26 mg m^{-3}) around 30 December, just before the water column was resampled (Station 57.02) on 31 December. Chl was undetectable by satellite during the ice-covered winter period in 2011, then increased again following the ice retreat in late 2011. Both blooms terminated just before the local ice advance. In the WAP, Chl was much lower, seldom exceeding 1 mg m^{-3} (Figure 3B). There were only 38 days with usable ocean color images available for the WAP compared to 112 for the ASP.

Total mass and organic carbon trap flux – ASP and WAP

During the full year (18 December 2010 to 18 December 2011) of sediment trap collection in the ASP, we captured parts of two flux events (“peaks”; Figure 2C) that exceeded $1000 \text{ mg m}^{-2} \text{ d}^{-1}$. Mass flux into the trap exceeded $118 \text{ mg m}^{-2} \text{ d}^{-1}$ (i.e., 10% of the peak observed flux) for 28 days in the first event, 18 December 2010 to 15 January 2011, and 42 days in the second event, 01 November – 13 December 2011 (Figure 2C). It is important to note, however, that we may have missed the beginning of the first event, and the end of the second, due to the limited deployment period. Multiple flux events, or bimodal (two peak) events are not unusual in our experience in the WAP, extending back to 1993. See, for example, the extended, two-peak event in 2010–2011 (Figure 3C). The maximum mass fluxes captured by the ASP sediment trap were 1001 (8 January 2011) and $1180 \text{ mg m}^{-2} \text{ d}^{-1}$ (22 November 2011) and thus 2–3 times greater than the corresponding peaks in the WAP (Figure 3C). The first flux peak in the ASP occurred one week after the Chl peak (08 January; Figure 2C). A secondary Chl peak on 14 February was not accompanied by a flux event. In 2011–2012 the peak mass flux preceded the period of high water column Chl by about a month (Figures 2B,C); however, the ice retreat was later and intermittent. Some ice cover ($< 20\%$) during this period (Figure 2A) may have either supported ice-algal production or interfered with satellite detection of an under-ice phytoplankton bloom. The total mass flux into the ASP trap, integrated from 18 December 2010 to 20 December 2011 was 44 g m^{-2} . Of this total, 31 g m^{-2} or 69% was contributed by the two flux events, over 60 days or 16% of the

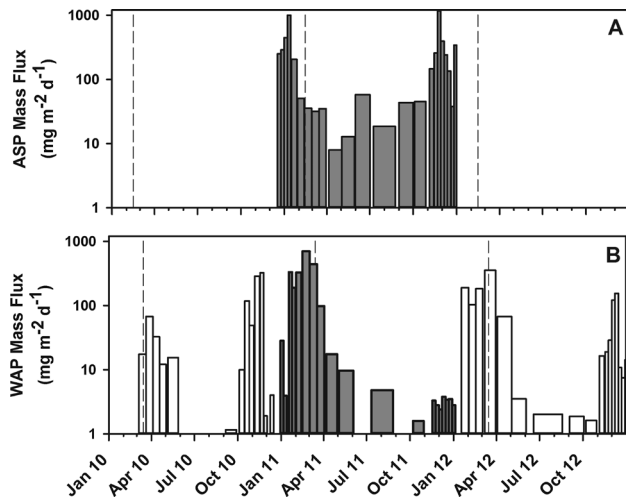


Figure 4
Mass particle fluxes in the ASAP and WAP.

Vertical mass fluxes of sinking particulate matter in the Amundsen Sea Polynya (A) and western Antarctic Peninsula (B) are plotted on log scale to reveal the low fluxes in winter (compare with Figures 2C and 3C). No visible bars in B indicates very low fluxes, not lack of samples. Bars for WAP fluxes in panel B during the ASPIRE sampling period are shaded similarly to bars in panel A to facilitate a temporal comparison between the data sets. Dashed lines as in Figs. 2, 3.

doi: 10.12952/journal.elementa.000046.f004

full year of collection. Sediment trap deployments in the WAP over the same period captured two flux peaks in 2010–2011 and one in 2011–2012 (Figure 3C).

Mass fluxes in the ASP were significantly larger than in the WAP during winter (May–September; Table 1). When plotted conventionally on a linear scale, the wintertime mass fluxes in the WAP were so low as to be invisible (Figure 3C); however a logarithmic scale (Figure 4) reveals low, but measurable mass fluxes throughout the winter.

Particulate organic carbon (POC) flux into the traps (Figure 5) reflected the mass fluxes (ASP POC ($\text{mmol C} = 5.34 * \text{Mass} + 0.16, r^2 = 0.82, n = 23$) and twice exceeded $\sim 5 \text{ mmol C m}^{-2} \text{ d}^{-1}$. During the two peak flux events described above, POC flux into the ASP trap exceeded $0.8 \text{ mmol C m}^{-2} \text{ d}^{-1}$ (i.e., 10% of the peak observed flux) for 28 and 14 days, respectively (Figure 5A). The maximum POC fluxes captured by the ASP sediment trap (Figure 5A) were $8 \text{ mmol C m}^{-2} \text{ d}^{-1}$ (peak 1, 18 January 2011) and $4.8 \text{ mmol C m}^{-2} \text{ d}^{-1}$ (peak 2, 22 November 2011). The total POC flux into the trap, integrated from 18 December 2010 to 20 December 2011 was $315 \text{ mmol C m}^{-2}$. Of this total, $149 \text{ mmol C m}^{-2}$ or 47% was contributed by the two flux events, over 42 days or 11% of full year of collection. The peak POC fluxes in the WAP were 2.5 and $2.1 \text{ mmol C m}^{-2} \text{ d}^{-1}$ in 2010–2011 and 2011–2012, respectively (Figure 5C), less than half the maximum POC fluxes during the same period in the ASP. The annual total POC fluxes at the WAP site were 189 and 173

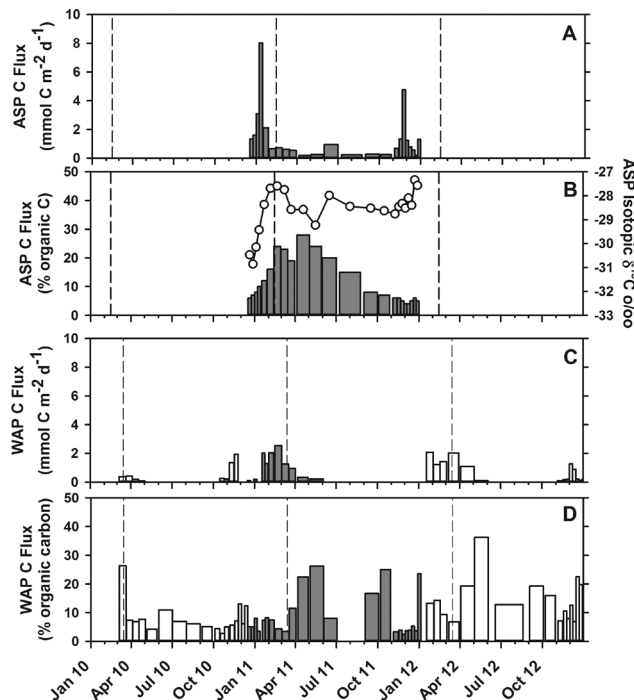


Figure 5
Particulate organic carbon fluxes in the ASP and WAP.

Bars indicate particulate organic carbon fluxes (A, C) and percent organic carbon content of the captured material (B, D) in the Amundsen Sea Polynya (A, B) and western Antarctic Peninsula (C, D). Panel B also shows the $\delta^{13}\text{C}$ of the POC flux in the Amundsen Sea (closed circles with connecting lines). Bars for WAP data in panels C and D during the ASPIRE sampling period are shaded similarly to bars in panels A and B to facilitate a temporal comparison between the data sets. No visible bars in C, D indicates very low fluxes, not lack of samples. Dashed lines as in Figs. 2, 3.

doi: 10.12952/journal.elementa.000046.f005

Table 1. Summary of seasonal fluxes into sediment trap sample cups in the western Antarctic Peninsula (WAP) and Amundsen Sea Polynya (ASP) during 2010–2011^a

Period	Statistics	POC flux (mmol C m ⁻² d ⁻¹)		Total mass flux(mg m ⁻² d ⁻¹)	
		WAP	ASP	WAP	ASP
Annual	Mean	0.48	1.38	96	229
	Std dev.	0.79	19.7	183	304
	N	23	22	23	22
	t-test	0.035		NS	
Winter	Mean	0.11	0.39	6.70	35.6
	Std dev.	0.15	0.31	7.01	19.1
	N	5	5	5	5
	t-test	NS		0.024	
Peak	Mean	1.62	2.94	271	503
	Std dev.	0.52	2.38	186	374
	N	11	8	11	8
	t-test	NS		NS	

^aPairwise t-test results indicate significance of comparisons between the ASP and WAP POC or mass fluxes in seasonal sampling intervals. NS: not significant ($p > 0.05$).

doi:10.12952/journal.elementa.000046.t001

mmol C m⁻². The POC flux contributions to each peak flux event were 111 and 131 m⁻² d⁻¹ or 59 and 76% of the annual POC fluxes. Thus, although peak fluxes in the ASP were more intense than in the WAP, a smaller fraction of the total annual ASP flux occurred during rapid settling events because of the higher wintertime fluxes there. The long term average annual (1992–2013) POC flux into the WAP trap is 193 ± 98 mmol C m⁻² (n=15, range 26–296). Several complete years are missing due to trap malfunction or loss.

Composition of the particle flux in the ASP and WAP

Molar C:N ratios averaged 7.6 ± 0.5 (n = 23) for the ASP samples (data not shown), indicative of fresh marine particulates throughout the sampling period. The long-term average for the WAP (1992–2013) is 8.3 ± 3.5 (n=877). The organic carbon content (% Corg) of the particle flux averaged $12 \pm 8\%$ (range of 4–28%, n=23) in the ASP, and $9 \pm 8\%$ (range of 3–26, n = 62 for 2010–2102) in the WAP (Figure 5B,D). The organic content was especially high in the ASP in early winter, when it ranged from 15 to 28%. Particulate matter in the ASP was generally depleted in ¹³C (Figure 5B). Samples collected during the first peak flux event were especially depleted, averaging -29.9 ± 1.0 ‰ (n = 5), then ranged from -27 to -29 over the rest of the collection period. Isotopic data are not available for the WAP samples. The nitrogen isotopic composition ranged from 0.9 to 9 ‰ (mean 3.2 ± 1.8 , n=22, neglecting a spurious value of 14 in the first sample cup). There was a significant correlation ($R = 0.59$, n = 14, $p < 0.05$) between % Corg and $\delta^{15}\text{N}$ for samples comprising the two peak flux events (Figure 6). Composition was highly variable in winter, possibly reflecting spatial patchiness of the biotic assemblages in the overlying sea ice, or a variable contribution from resuspended sedimentary material transported laterally to the trap site.

Contribution of zooplankton fecal pellets to the particle flux

Microscopic examination of the particle samples collected in the sediment trap revealed that the flux was usually dominated by amorphous phytodetritus or fluff (Figure 7). Large diatom frustules were not apparent, consistent with cruise observations that the phytoplankton bloom in 2010–2011 was heavily dominated by *Phaeocystis* colonies (Alderkamp et al., 2015). Some fecal “strings” from the ice krill *E. crystallarophias* and large calanoid copepod *C. acutus* were apparent during the early part of the first peak, and prior to the second. However the samples comprising the first peak flux event appeared to be dominated by smaller fecal pellets from mid-sized copepods such as *M. gerlachei* (Figure 7B). All three species were among the dominant taxa during our cruise. Following the first peak flux event, and during the winter, the flux was dominated by phytodetritus, but included contributions from a diverse assemblage of fecal pellet types (Figures 7C, D).

Fecal pellet production rates varied by species and date, ranging from 0 to 20 pellets per individual per day (Figure 8). Measured fecal pellet production rates and fecal pellet carbon content (data not shown) were combined with zooplankton abundances from MOCNESS tows (Wilson et al., 2015) to yield potential pellet POC fluxes (Table 2). *E. crystallarophias* did not produce any fecal pellets on 26 December but produced many more during the experiment on 05 January to generate an overall average of 0.052 ± 0.047 mmol C

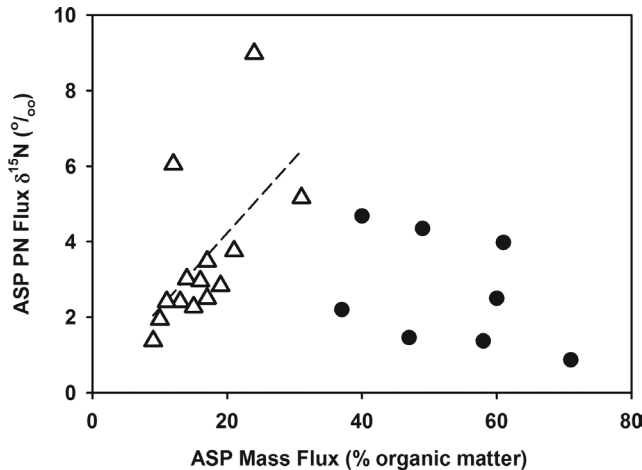


Figure 6
Organic carbon and ¹⁵N content of particle flux.

Open triangles indicate data from samples during the peak flux periods (29 December 2010 to 22 January 2011 and 16 September to 23 December 2011). Closed circles indicate data from samples during non-peak flux periods. The dashed regression line is for data from the two peak flux periods ($r^2 = 0.35$, $p < 0.05$, $n = 14$).

doi: 10.12952/journal.elementa.000046.f006

$\text{ind}^{-1} \text{day}^{-1}$ ($n = 3$). Zooplankton fecal pellet production potentially contributed 15–189% of the estimated carbon export from the surface layer (Table 3; see Discussion). At Station 66 we detected a super swarm of *E. crystallarophias* with the Metro net (Wilson et al., 2015). This vast swarm potentially could have contributed up to $128 \pm 59 \text{ mmol C m}^{-2} \text{ d}^{-1}$ to POC flux in the ASP, but such a contribution was not reflected in the trap samples. In the WAP, the flux tends to be dominated throughout the year by fecal material, especially krill pellets (Gleiber et al., 2012).

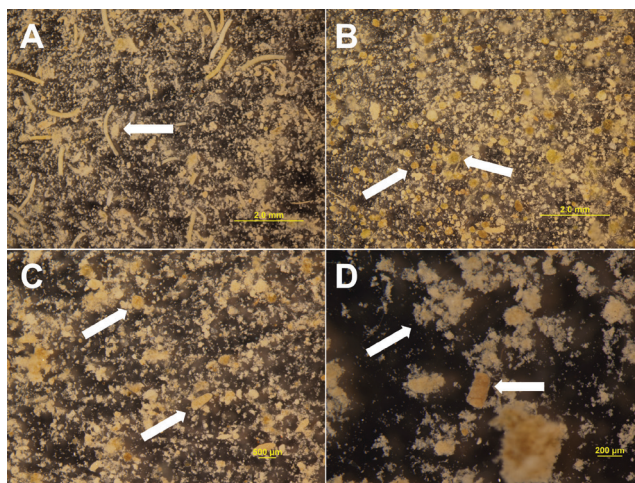
Discussion

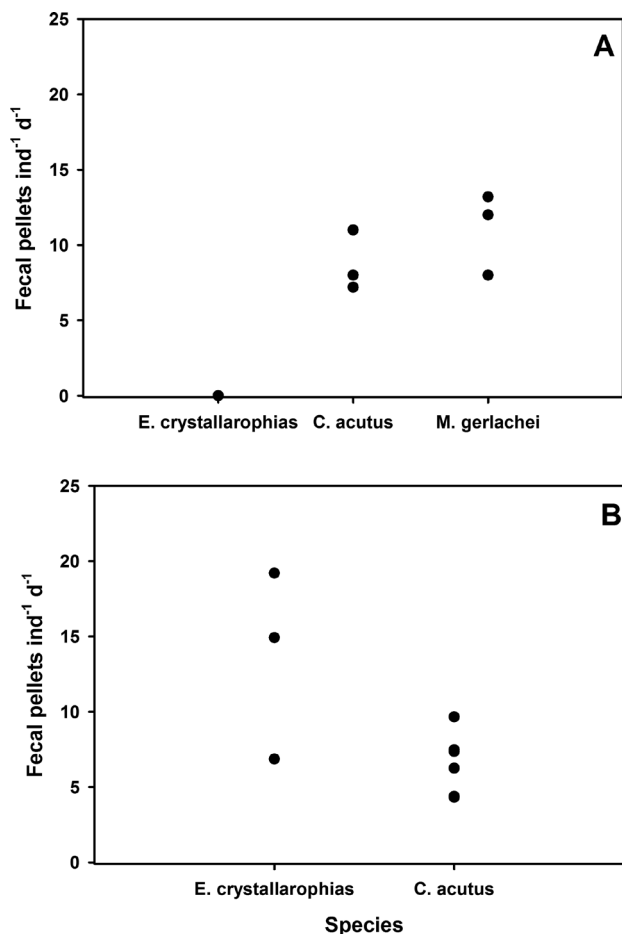
When viewed together, the results from ASPIRE suggest dividing the year of flux observations into three phases (Table 4): two brief flux events (28 and 14 days when flux $> 0.8 \text{ mmol C m}^{-2} \text{ d}^{-1}$, Figure 5) and an intervening, relatively low but non-zero flux period extending from midsummer (late January 2011) through the winter period of heavy ($> 50\%$) ice cover. The two flux events contrasted in several ways. The first peak we measured occurred in the summer, entirely after the ice retreat, in open water (0% ice cover). The second peak appeared to commence in the late winter–spring (September–November) and was perhaps related to the high sea ice algal productivity found in this region (Fransson et al., 2011; Arrigo et al., 2014). It started before the full ice retreat, and proceeded under ice cover averaging $13 \pm 15\%$. The two peaks had similar mean fluxes when scaled over the time of each event, but they differed in their organic and isotopic composition. The winter–spring peak had a greater contribution from fecal pellets, whereas the summer peak was dominated by phytodetritus. Zooplankton fecal pellet production contributed about 10–40% of the export from the upper 100 m during the summer flux peak (Table 3). Both flux peaks were dynamic and changed in composition during their relatively brief occurrence. In the Discussion below, we first address some of the uncertainties and biases in trap collection and difficulties of comparison between the two regions (with

Figure 7
Images of sediment trap samples.

Sample 1, from 18 December 2010 near start of first flux event, shows *Euphausia crystallarophias* (arrow) and *Calanoides acutus* pellets (both cylindrical) in a sample dominated by amorphous aggregates of phytodetritus, at magnification of 19.2X (A). Sample 4 from 8 January 2011 at peak of first flux event was composed primarily of numerous smaller (50–200 μm) copepod fecal pellets likely from *Metridia gerlachi* (arrows), also shown at magnification of 19.2X (B). Sample 13, from 01 July 2011 in midwinter, was composed predominantly of amorphous phytodetritus with copepod and larvacean pellets (arrows), shown at magnification 30X (C). Sample 18, from 22 November 2011 at peak of second flux event, was dominated by phytodetritus (left arrow) with fecal pellets (right arrow) of unknown origin (possibly fish), shown at magnification of 48X (D).

doi: 10.12952/journal.elementa.000046.f007



**Figure 8**

Experimental measurements of zooplankton fecal pellet production rates.

Incubations were conducted with specimens of *Euphausia crystallarophias*, *Calanoides acutus*, and *Metridia gerlachei* collected on 29 December 2010 (A) and collected on 05 January 2011 (B) to determine number of fecal pellets produced per individual (ind.) per day.

doi: 10.12952/journal.elementa.000046.f008

two different trap designs). We then address seasonality of the flux events, and discuss their evolution and origins. Next, we interpret the ASP particle fluxes in the context of net primary production (NPP) and net community production (NCP) rates in the ASP system. Finally, the paper concludes with a brief assessment of caveats and future research priorities.

Interpretation of moored sediment trap data

Moored sediment traps have two distinct advantages over alternative methods for deriving estimates of marine particle flux and export. They provide a collection of the sinking particle assemblage for subsequent physical, chemical and biological analyses; and they often provide the only year-round *in situ* biogeochemical information of any kind for remote locations such as Antarctica. Moored traps are subject to several kinds of

Table 2. Zooplankton abundance in the Amundsen Sea Polynya, December 2010 to January 2011, and fecal pellet carbon production rates

Station	Date	<i>Euphausia crystallarophias</i>	<i>Calanoides acutus</i>	<i>Metridia gerlachei</i>	<i>E. crystallarophias</i>	<i>C. acutus</i>	<i>M. gerlachei</i>	Potential flux
		(Individuals m ⁻²)			(mmol C m ⁻² d ⁻¹)			
13	19 Dec 2010	138	3320	609	7.17	2.17	0.03	9.33
25	22 Dec 2010	53	921	419	2.75	0.58	0.02	3.42
35	25 Dec 2010	45	1396	285	2.33	1.83	0.02	3.25
50	29 Dec 2010	107	2266	203	5.58	1.42	0.01	7.08
57	3 Jan 2011	21	4007	228	1.08	2.58	0.01	3.67
Mean								4.67
St. dev								2.92

doi: 10.12952/journal.elementa.000046.t002

Table 3. Sources of vertical particle flux exiting the upper 100 m in the Amundsen Sea Polynya, December 2010 to January 2011

Station	Date	NCP ^a	Export ^a	Fecal pellet flux ^b
		(mmol C m ⁻² d ⁻¹)		
13	19 Dec 2010	28.5	4.9	9.33
25	22 Dec 2010	47.3	8.5	3.42
35	25 Dec 2010	53.3	14.3	3.25
50	29 Dec 2010	49.2	13.5	7.08
57	3 Jan 2011	53.4	23.9	3.67
Average		46.3	13.0	5.35

^a NCP and export rates from P. Yager (personal communication) were converted to daily rates using the days since first day of 50% ice cover. Export is average of high and low estimates provided by P. Yager (personal communication).

^b Fecal pellet flux estimates used zooplankton stocks from Wilson et al. (2015) and fecal pellet production rates in Table 2

doi:10.12952/journal.elementa.000046.t003

bias, however, that can affect flux estimates. These effects, notably interference from sample-contaminating live zooplankton “swimmers” and horizontal current shear over the trap opening, are most pronounced in the upper 200 m. Swimmers that actively enter a sediment trap collection cup with preservative will die in the cup and add to the collected material, falsely increasing the apparent flux unless recognized and removed.

The effects of trap hydrodynamics are more complicated, but well studied. A moored (stationary) trap in a moving current will generate shear and turbulence across the trap opening that can advect water and particles into or out of the trap (Gardner, 1980; Butman et al., 1986; Gust, 1992; Buesseler et al., 2007a). Traps may over- or under-collect relative to independent calibration methods (Buesseler, 1991). Results of theoretical treatments, controlled laboratory flume studies and field comparisons all suggest that hydrodynamic bias increases with current speeds > 5–10 cm sec⁻¹, and with decreasing trap height:diameter (aspect) ratio. Trap shape also affects collection efficiency, with conical traps performing less well than cylindrical designs. The WAP trap is conical with an aspect ratio of 1.8 (164:91 cm) and was deployed at 170 m. The new cylindrical trap we deployed in the ASP was designed to minimize hydrodynamic bias, has an aspect ratio of 4.8 (192:40 cm) and was deployed at 350 m. To further evaluate possible differences between trap collections, it is necessary to consider the physical current regime in the two areas.

Table 4. Summary of environmental and biogeochemical observations characterizing seasonality of sediment trap collections, December 2010 to December 2011, in the Amundsen Sea Polynya

Event	Dates (or days)	Mean values for period					
		Ice cover (%)	POC flux (mmol C m ⁻² d ⁻¹)	Mass flux (mg m ⁻² d ⁻¹)	%orgC (%)	δ ¹³ C (‰)	Composition
Peak 1							
Ice retreat date	18 Nov 2010						
Peak start date	18 Dec 2010	0	3.3	438	9	-29.86	fecal pellets & phytodetritus
Peak end date	15 Jan 2011						
Peak duration (days)	28						
Low flux/winter							
Start date	15 Jan 2011						
Ice advance date	26 Feb 2011	53	0.5	44	17	-28.34	fecal pellets & phytodetritus
End date	11 Nov 2011						
Duration (days)	293						
Peak 2							
Peak start date	15 Nov 2011						
Peak end date	29 Nov 2011	19	2.0	528	5	-28.35	phytodetritus
Ice retreat date	06 Dec 2011						
Peak duration (days)	14						

doi:10.12952/journal.elementa.000046.t004

The ASP region is characterized by complex bathymetry, an irregular coastline, several ice tongues and shelves, glacial inputs of freshwater and an abrupt shelf break, all of which contribute a complicated and variable circulation regime (Randall-Goodwin et al., 2015). The sediment trap mooring site receives both inflows of Circumpolar Deep Water from offshore, and outflows from under the ice shelf. Currents near the ASP trap, measured by the ship's hull-mounted acoustic Doppler current profiler in the trap region north of the DIS, showed that at the time of the 2010–2011 flux peak, currents were weak, averaging about 5 cm sec^{-1} (Randall-Goodwin et al., 2015). These measurements of local currents, although limited to the time of the cruise, suggest minimal bias in the ASP particle fluxes during at least one of the peak flux periods.

Both observations (Savidge and Amft, 2009) and models (Piñones et al., 2011) indicate that long-term, depth-averaged (0–200 m) currents in the WAP trap region are also generally $\sim 5 \text{ cm sec}^{-1}$ or less, at the lower end of the threshold current speeds causing bias in trap collections. Nonetheless Thorium-234 calibration (Buesseler et al., 2010) suggests that the WAP trap may be under-collecting, at least at some times. In view of these considerations we expect that the ASP trap should be more efficient (i.e., less likely to under-collect) than the WAP trap. We cautiously conclude that although differences between particle flux estimates in the ASP and WAP may be due in part to differences in trapping efficiency caused by the trap designs and their interactions with the ambient current regimes, they are also likely to be due to real regional differences in productivity and export.

Using moored traps to estimate export from the surface layer is also sometimes problematic. Sinking particles can disintegrate into suspended particles and be consumed or decomposed as they settle downward toward the traps (Banse, 1990; Kellogg et al. 2011; Giering et al., 2014). Accordingly, flux estimates at depth must be extrapolated to the export value at the base of the surface source layer (usually 100 m; Martin et al., 1987), if no independent estimate is available. The issue of extrapolation and the extent and functional form of flux attenuation with depth has received great attention in the literature (e.g., Najjar et al., 1992; Armstrong et al., 2001; Francois et al., 2002; Henson et al., 2012). To address the issue of flux attenuation, we used independent estimates of NCP (the ultimate source of particle flux to depth) and the actual export rate from the upper 100 m (Yager et al., 2014). These estimates are discussed below, along with consideration of the roles of bacteria and zooplankton in reducing the particle flux as it settles through the water column between the surface layer and the trap depth.

Seasonality and evolution of the annual flux events

Particle flux in Antarctic waters, especially in the sea ice zone, is emphatically seasonal (Fischer et al., 1988). Ducklow et al. (2008), using the long-term (1993–2007) WAP dataset, showed that on average 85% of the annual particle flux was contained in the annual flux peaks. “Peaks” were defined as periods when the flux exceeded $0.2 \text{ mmol C m}^{-2} \text{ d}^{-1}$, a criterion that resulted in long ‘tails’ on the flux profiles. For the ASP, this low threshold would place the entire year in the peak, so we used a more stringent value of $0.8 \text{ mmol C m}^{-2} \text{ d}^{-1}$, which makes the peak events shorter. Even so, the average peak in the LTER dataset (1993–2013) contributed 59% of the annual flux in just 52 days, or 14% of the year, a 4.2-fold enhancement ratio. In 2010 and 2011, the WAP peaks were 59 and 76% of the total.

Keeping in mind that there is just one year of observations, the ASP data suggest a somewhat different picture. The extreme seasonality is apparent (Figure 2); however the peaks are brief and superimposed on a relatively high background flux, compared to the WAP observations. The two peaks each contributed 33 and 14% of the annual total, although they did so during only 7 and 3% of the year (both with a 4.7-fold enhancement ratio). Thus, even these very brief flux events contribute a disproportionate fraction of the annual flux. We caution that the higher background flux in the ASP could be in part a consequence of higher trapping efficiency of the Technicap sediment trap, compared to the traps deployed in the WAP.

Three key observations characterize the summer flux event: it occurred virtually simultaneously with the surface phytoplankton bloom (Figure 2); it was initially very depleted in ^{13}C (Figure 5); and large fecal “strings” were conspicuous (Figure 6A), although the flux was visually dominated by phytodetritus. The rapid growth of the surface bloom to very high chlorophyll concentration ($10\text{--}20 \mu\text{g L}^{-1}$; Figure 2; see also Figure 2 in Yager et al., 2012, page 42) suggests that krill grazing, even with ice krill (*Euphausia crystallographias*) present (Wilson et al., 2015) and producing pellets (Table 2, Figure 8), was not a limiting factor on bloom initiation. This conclusion is consistent with the observed dominance of the bloom by *Phaeocystis antarctica*, which is not a preferred food choice of krill and other grazers, at least in its colonial stage (Leventer and Dunbar, 1996). Furthermore the highly depleted ^{13}C of the earliest flux values argues against a significant contribution from fecal pellets. Fischer (1991) showed that krill fecal pellets were enriched by 3–4 ‰ relative to their phytoplankton origin. Zooplankton preferentially respire lighter carbon, leaving their biomass and unassimilated fecal egesta heavier (McConnaughey and McRoy, 1979). The low (more depleted) $\delta^{13}\text{C}$ measured in the initial samples is likely due to a phytoplankton response to high aqueous CO_2 concentrations in cold water (Rau et al., 1989) and to the isotopic composition of the respiratory component of the winter CO_2 , which is expected to be depleted. Pre-bloom Winter Water (WW) $p\text{CO}_2$ and DIC values for this region are $455 \mu\text{atm}$ (Mu et al., 2014) and $2215 \mu\text{mol C kg}^{-1}$ (Yager et al., 2014). Later in the cruise period (January), following significant

photosynthesis and warming, $p\text{CO}_2$ and DIC declined to $< 200 \mu\text{atm}$ and $2041 \mu\text{mol kg}^{-1}$ (Mu et al., 2014), which would enrich the organic carbon of the phytoplankton, as we observed. In our samples, isotopic ratios increased steadily throughout the first flux event, from initial values of ca. -30.5 to -27.6‰ at the end of the flux event in February. The particles became increasingly enriched as the bloom progressed, also consistent with increasing grazing pressure and the higher abundance of diverse fecal pellets in later samples (Figure 7BC). The relationship between the organic carbon and ^{15}N content (Figure 6) also suggests that increasing Corg content during the peak flux events was driven by contributions from zooplankton fecal output, as opposed to a declining contribution from phytoplankton. Our combined observations suggest that the 2010–2011 phytoplankton bloom in the ASP was terminated by rapid mass sedimentation of phytoplankton aggregates combined with increasing zooplankton grazing in late January 2011.

During the first peak flux period, Corg constituted $\sim 15\%$ of mass, so organic matter contributed about 40% of the total mass flux. Results from short-term floating traps deployed in this region during the ASPIRE cruise suggested that a large portion of the other 60% of the total mass could have been terrigenous particles resulting from resuspension, lateral advection over a few kilometers, and deposition into the traps (R. Sherrell, unpublished). Unfortunately, our knowledge of the second flux peak in November–December 2011 is limited, as no research vessels occupied the region at that time. High production and grazing (or sloughing) of sea ice algae, observed during previous years in this region (Fransson et al., 2011) and also in the sea ice covered areas north of the ASP in 2010–2011 (Arrigo et al., 2014) would be consistent with this early season flux beneath the sea ice. Indeed, ASPIRE observations of high POC inventories and large krill populations associated with marginal sea ice Station 66 on the northern edge of the ASP (Wilson et al., 2015; Yager et al., 2014) may offer insight for the springtime flux we observed the following year.

Kim et al. (2014) present sediment trap observations overlapping ours in time, but from the zone of persistent 40–100% sea ice cover 250 km northwest of the central ASP (Figure 1). They observed one peak in early 2011, but did not see a second peak at the end of the year. The timing and pattern of their flux events were similar to ours, but the magnitude of the flux was lower and the event lasted longer. Their peak coincided with the annual period of low ($\sim 40\text{--}50\%$) sea ice cover in January–March 2011. They concluded from opal (biogenic silica) data that the particle flux in their region was dominated by diatoms rather than *Phaeocystis antarctica*; but they also observed from isotopic data that there was an increasing contribution from zooplankton when the organic content was greater. They did not observe the highly depleted carbon isotopic values that we observed (-26.1 to -27.9), possibly indicating the lack of an intense phytoplankton bloom in the SIZ region. Because Kim et al. (2014) employed a conical trap (the same as our WAP trap), the absence of a second peak may be explained by collection bias and/or lateral advection.

The ASP flux events in 2010–2012 were brief, at least when viewed in relation to WAP observations. However the WAP results come from a lower latitude (64°S) area with a much shorter period of ice cover (and longer open water period) than the ASP. More comparable observations come from moored sediment trap deployments in the Ross Sea Polynya (RSP) at similar latitude (Collier et al., 2000). Like the ASP, sea ice cover in the RSP lasts about 250 days with a 100-day open water period extending from late November–early December until mid-March. The annual phytoplankton bloom in the RSP is typically dominated by *Phaeocystis*. Collier et al. (2000) deployed conical time series sediment traps at 206 m and 481 m in a 565-m deep water column on the mid-continental shelf in the Ross Sea from 28 November 1996 to 10 January 1998. They observed an annual flux event that was both longer in duration and shifted in time compared to our observations in the ASP. The flux peak lasted 145 days, averaged $41 \text{ mg m}^{-2} \text{ d}^{-1}$ and contributed 78% of the annual flux (an enhancement ratio of only about 2). The peak flux event did not start until late January but it lasted until early June. The maximum flux occurred in May, with most of the peak flux occurring under 80–100% ice cover. This flux event was similar to the WAP in its duration and proportion of the annual flux contained in the peak event, but it was more similar in magnitude to the ASP; its phenology (timing) differed from both in regard to season and ice cover. Although it was tempting to conjecture that the brief flux events in the ASP were related to the brief period of open water and a truncated bloom, the fact that one of the ASP flux events occurred mostly under the ice, and the flux events in the RSP were long, led us to abandon this idea. The Ross Sea observations also suggest the possibility of a pronounced lag or uncoupling between the periods of maximum surface productivity and particle flux.

Our experience in the WAP also reminds us that the most important conclusion about sea ice cover and biogeochemical fluxes in Antarctic waters is their great interannual variability (Ducklow et al., 2007). The ASP exhibits extremely high interannual variability in ocean color (Arrigo and van Dijken, 2003; Arrigo et al., 2012). Very long and very short, and large and small peaks have been observed over twenty years in the WAP. Our observations in the ASP are limited to a single year. There are more observations in the Ross Sea, but not enough to generalize. These caveats notwithstanding, the annual flux in the ASP, $315 \text{ mmol C m}^{-2}$, was greater than all but one of 16 years sampled in the WAP. The maximum flux in the ASP, $8 \text{ mmol C m}^{-2} \text{ d}^{-1}$, was greater than all but two flux peaks observed over 22 years in the WAP. However, as noted above, we cannot rule out trap bias (under-collection by the conical traps used in the WAP and RSP) as an influence on this comparative result.

Table 5. Particle flux into moored sediment trap, 21 December 2010 to 11 January 2011, and differences between particle flux sources exiting 100 m (NCP, Export) and delivery at trap depth^a

Sample	Date	Flux to Trap mmolC m ⁻² d ⁻¹	Δ flux (NCP - Trap) mmolC m ⁻² d ⁻¹	Δ flux (Export - Trap) mmolC m ⁻² d ⁻¹
Trap (350 m)	21 Dec 2010	1.93	45.4	6.6
Trap (350 m)	28 Dec 2010	1.58	47.6	11.9
Trap (350 m)	4 Jan 2011	3.08	50.3	20.8
Trap (350 m)	11 Jan 2011	8.00	n/a	n/a
Average		3.65	47.8	13.10

^an/a indicates not available.

doi:10.12952/journal.elementa.000046.t005

Sources and sinks for Amundsen Sea particle flux

The export flux in the open sea ultimately derives from primary production. The amount of net primary production (NPP) remaining after zooplankton and bacterial respiration, the net community production (NCP), is available for export and for storage in longer-lived upper trophic level predators. A variable fraction of the NPP and NCP is in the form of dissolved organic matter and, hence, not captured in sediment traps (Hansell, 2002). NCP was estimated at each major ASP sampling station from the inventory of total dissolved inorganic carbon (DIC) in the upper 100 m (Yager et al., 2014). The difference between the winter DIC and that observed at each station in midsummer (Δ DIC) is the cumulative NCP from the start of the growing season to the sampling date, including both net particle and DOC production. Our cruise took place while the trap mooring site was entirely in open water, and during the first four trap sampling intervals, including most of the first peak flux event (Figure 2). To obtain daily rates for comparison with the particle flux into the trap, we assumed that NCP started to accumulate on the day sea ice cover first fell below 50% (Yager et al., 2014) and continued until the date of sampling, yielding the NCP rates shown in Table 3. NCP averaged 46.3 ± 10.3 mmol C m⁻² d⁻¹ within the polynya over the cruise period. The net air-sea CO₂ exchange can also be used as an estimate of the NCP. Mu et al. (2014) estimated that 44.4 ± 15.5 mmol CO₂ m⁻² d⁻¹ was absorbed in the productive, open central ASP during the cruise period, in good agreement with the Δ DIC-based value. The average net primary production measured with ¹⁴C incubations during our cruise was high, 228 ± 71 mmol C m⁻² d⁻¹ (Yager et al., 2014). The NCP was thus about 20% of the measured NPP, a reasonable value (Quay et al., 2010). The NCP was much greater, however, than the particle flux arriving at the sediment trap (Table 5).

Not all of the Δ DIC-based NCP was exported during the brief cruise period on which these estimates are based. Some of the fixed carbon accumulated as POC, DOC and macrozooplankton biomass in the upper 100 m (Yager et al., 2014). We used the difference between the NCP and the accumulated carbon stocks as an estimate of the amount of production actually exported during the cruise period, which also approximates the first peak flux event. This method gave 100-m export estimates of 4.9 – 23.9 mmol C m⁻² d⁻¹ for five stations within the ASP (Table 3), or about 10% of the NPP. Floating sediment traps at 60 and 150 m, deployed 31 December–03 January (Station 57), gave export fluxes of $\sim 26.6 \pm 2.1$ and 2.7 ± 0.8 mmol C m⁻² d⁻¹ at 60 and 150 m, respectively (P. Yager and R. Sherrell, unpublished). These results indicate active remineralization of the POC flux between 60 and 150 m. These 60-m floating trap estimates of export are greater than the 100-m export values in Table 3, consistent with this conclusion. The floating trap estimates for POC flux at 300 m were 1.5 ± 1.4 mmol C m⁻² d⁻¹, similar to the moored trap values (Table 5). The trap results thus suggest that most of the carbon flux attenuation between the euphotic zone and the 350-m trap depth occurred in the upper 150 m, consistent with previously described power law relationships between POC flux and depth, based on sediment trap studies in a variety of oceanic regimes (Berelson, 2001).

Here we use observations on bacterial production rates (Williams et al., 2015) and macrozooplankton stocks (Wilson et al., 2015) to estimate the amount of respiration potentially occurring in the 50–350 m depth interval, and compare it to the observed decline in the particle flux. We assumed that all bacterial production below ~ 50 m was dependent on particle flux originating in the euphotic zone. This assumption represents an overestimate, because some of the subeuphotic zone bacterial production is based on DOC exported from the surface; however DOC export is generally observed to be very low in Antarctic seas (Hansell, 2002). It also leads to an overestimate if some of the NCP in the overlying water column was advected and lost to the column below (see below). Depending on the assumed values for the leucine to bacterial production conversion factor and the bacterial growth efficiency, bacterial respiration in the 50–350 m depth layer was between 15 and 116 mmol C m⁻² d⁻¹ (Table 6). The minimum value of the cumulative 50–350 m bacterial respiration is about the same as the average loss of exported material in the same depth range (13 mmol C m⁻² d⁻¹; see Δ flux, export - trap, in Table 5). This similarity suggests that bacteria in the upper 350 m could have remineralized most of the POC export flux. In contrast, zooplankton respiration, and associated disaggregation of the particle flux, was small. Macrozooplankton respiration rates were estimated to be 5% of the

Table 6. Bacterial production and respiration in the Amundsen Sea Polynya at 50–350 m

Depth (m)	Leucine incorporation rate ($\mu\text{mol m}^{-2} \text{d}^{-1}$)	Bacterial production ^a		Bacterial respiration ^b	
		Low	High	Low	High
		($\text{mmol C m}^{-2} \text{d}^{-1}$)			
50–100	21.7	0.91	2.72	9.1	68
100–150	10.2	0.43	1.28	4.2	32
150–350	5.09	0.21	0.64	2.1	16

^a Production estimates are based on leucine incorporation data from Williams et al. (2015), using a conversion factor of 0.5 kg C mole⁻¹ leucine incorporated (Giering et al., 2014) for low estimates and 1.5 kgC mole⁻¹ leucine incorporated (Ducklow et al., 2000) for high estimates.

^b Respiration was estimated using bacterial growth efficiencies of 0.04 for high estimates and 0.10 for low estimates (Giering et al., 2014).

doi: 10.12952/journal.elementa.000046.t006

standing stock per day (Ikeda and Mitchell, 1982; Salliey et al., 2013), yielding rates of $< 0.01 \text{ mmol C m}^{-2} \text{d}^{-1}$ (Table 7). The same parameterization together with microzooplankton standing stocks for the 150–300 m layer ($0.9 \pm 0.5 \text{ mmol C m}^{-2}$; P. Yager et al., 2014) yields a respiration estimate of $\sim 0.05 \text{ mmol C m}^{-2} \text{d}^{-1}$, slightly greater than macrozooplankton respiration, but insufficient to make much impact on the sinking flux.

Finally, directly measured rates of community respiration (CO_2 production) at 150–300 m gave rates of $0.25 \mu\text{mol C L}^{-1} \text{d}^{-1}$ (Williams et al., 2015). This rate converts to $38 \text{ mmol C m}^{-2} \text{d}^{-1}$ for the 150–350 m layer, consistent with the bacterial respiration and more than sufficient to consume the export leaving the surface layer (Table 5).

Recently Giering et al. (2014) presented a balanced carbon budget for the upper 1000 m at a site in the North Atlantic. They showed that bacterial respiration was responsible for decomposing 70–90% of the export flux, and they postulated that the principal role of zooplankton was to fragment and disperse sinking particles, both making them more vulnerable to bacterial attack and converting larger sinking particles into smaller, suspended ones. Our results are consistent with theirs: most (nearly all) the particle decomposition was due to bacterial activity, and it could account for a majority of the decline in flux between 50–100 and 300–350 m. Our results are also consistent with recent data from Arctic seas, where a significant attenuation of the export flux has been attributed to microbial decomposition of sinking particles (Kellogg et al., 2011, 2014).

Other considerations

The 1-dimensional argument above neglects horizontal advection as a mechanism for particle export, or inputs, to the trap vicinity. The distance travelled by particles from their source region depends on their sinking rates as well as horizontal current speeds (Siegel and Deuser, 1997). Particles sinking at $1\text{--}5 \text{ m d}^{-1}$ in a current field averaging $5\text{--}10 \text{ cm sec}^{-1}$ (Ha et al., 2014) would travel horizontally about $5\text{--}10 \text{ km d}^{-1}$, or at least 200 km in the ca. 40–200 days that they would take to settle between 100 and 350 m. Larger and denser particles like fecal pellets sinking more rapidly at $10\text{--}100 \text{ m d}^{-1}$ would remain in the source region

Table 7. Macrozooplankton biomass and respiration in the Amundsen Sea Polynya at 150–350 m

Station	Dates	Biomass ^a (mmol C m^{-2})	Day or night	Respiration ^b ($\text{mmol C m}^{-2} \text{d}^{-1}$)
13	Dec. 18–19, 2010	0.05	N	< 0.01
13	Dec. 18–19, 2010	0.05	D	< 0.01
25	Dec. 22, 2010	0.01	D	< 0.01
25	Dec. 22, 2010	0.03	N	< 0.01
35	Dec. 25–26, 2010	0.02	D	< 0.01
35	Dec. 25–26, 2010	0.02	N	< 0.01
50	Dec. 29, 2010	0.10	N	< 0.01
50	Dec. 29, 2010	0.08	D	< 0.01
57	Dec. 31, 2010 – Jan. 2, 2011	0.11	N	< 0.01
57	Dec. 31, 2010 – Jan. 2, 2011	0.10	D	< 0.01

^a Zooplankton biomass data are taken from Wilson et al. (2015).

^b Respiration was estimated as 5% of the biomass per (24-h) (Ikeda and Mitchell, 1982; Salliey et al., 2013)

doi: 10.12952/journal.elementa.000046.t007

and generally be captured by the traps. For horizontal advection to be net source or sink from some area, there must be a spatial gradient in the particle field and production rates. If particle fields are uniform over large distances, horizontal advection cannot be invoked as a mechanism for adding or removing particles to or from a fixed location over a moored trap. Summer polynyas, however, are hotspots of elevated biomass and production, so that horizontal advection could act to transport particles from the high productivity polynya into the surrounding ice-covered, lower productivity region. Advection could also have the opposite effect, transporting water with a lower particle load from outside the polynya into the trap region.

Circulation in the ASP (Randall-Goodwin et al., 2015) supports the possibility of sediment resuspension and horizontal advection having a role in the ASP carbon budget. Prevailing southeasterly winds blow from the Thwaites Ice Tongue across the trap location driving locally produced ice (and water and particles) northwards. Circumpolar Deep Water enters the area from offshore, with low particle loads. An iron-rich, but organic particle-poor outflow from under the Dotson Ice Shelf also flows into the area (Figure 1, R. Sherrell, unpublished). All of these processes have the potential to affect the particle catch in the trap relative to local production at the surface. R. Sherrell (unpublished) observed that the vertical fluxes of trace metals and tracers of sedimentary inputs such as aluminum into floating sediment traps *increased* between 150 and 300 m, suggesting that a lateral, subsurface source of resuspended sediments was enhancing the mass flux to depth in the ASP. However, as noted above, the flux of particulate organic matter *decreased* between the same depths. Thus it is likely that resuspended material, possibly sourced from the shallow sediments surrounding the Martin Peninsula just to the west of the moored trap site, contributed substantial inorganic material but likely little organic material during the flux peak.

Addressing the problem of advection of the particle field, and how it impacts the apparent export rate, would require deployment of an array of sediment traps and current meters throughout the polynya region. Kim et al. (2014) observed an annual POC flux similar to ours at a site 250 km to the northwest, in the sea ice zone outside the ASP, an area covered by sea ice throughout the year. Primary production in the SIZ region averaged $17 \text{ mmol C m}^{-2} \text{ d}^{-1}$ in December 2010 and January 2011 (Lee et al., 2012), about 10% of the values inside the ASP. Surprisingly, given this lower NPP level, they observed fluxes comparable to the highly productive central ASP (see above). One explanation for this contrast is that some of the particle flux in the surrounding SIZ region could have been derived from the high productivity central ASP. However Kim et al. (2014) argue on the basis of sample composition that the material was derived from locally-produced, rapidly-sinking particles, and not advected from the central ASP.

Weston et al. (2013) reported a large difference between surface production and trap flux at 200 m for a moored (conical-type) sediment trap deployed in 2005–2006 in Marguerite Bay ($67.56^\circ\text{S}, 68.23^\circ\text{W}$), 350 km south of the WAP trap. They observed high new production rates in their study area, but with just 1% arriving in the traps (*cf.* 3–28% in ASP; Table 3). They speculated that most of the particulate organic matter leaving the surface layer was decomposed and regenerated as it settled through the water column, and characterized the region as “high recycling, low export.” However, Marguerite Bay is a region of locally high productivity in the WAP region with complex circulation; therefore some of the discrepancy could also be due to local advection into and/or away from the trap location.

We can assess trap flux in the central ASP by estimating the scaling factor for flux (F) attenuation between the surface production layer (50–100 m) and the trap depth (Martin et al., 1987). Martin et al. (1987) described flux profiles in the North Pacific using the empirical power function:

$$F_z = F_{100}[(Z/100)^{-b}] \quad (1)$$

where Z is the trap depth, F_{100} is the flux at a reference depth (here, the 100 m source depth) and b is the scaling factor by which we can compare flux attenuation at different sites. We use the estimate of $78 \text{ g C m}^{-2} \text{ d}^{-1}$ from Arrigo et al. (2012) for the mean annual primary production rate in the ASP (range of 61–94). Assuming an annual export ratio (NCP/NPP) of 0.20 gives a mean annual export production of 1.3 mol C m^{-2} (range of 1.0–1.6). The annual POC flux to the trap was $315 \text{ mmol C m}^{-2}$ ($0.32 \text{ mol C m}^{-2}$), which yields a b value of 1.1 (range of 0.9–1.25). This value falls within the range of open ocean b values (0.60–1.24) derived by Berelson (2001), but is on the high side of the range of 0.77–1.04 for the Southern Ocean. These scaling lengths agreeing with previous values suggest that much of the particle flux in the central ASP was respired by microbial activity between 100 and 350 m. Microbial decomposition of the particle flux renders the biological pump in the ASP system somewhat less efficient, compared to some other ocean ecosystems, as a source of carbon export to greater depths where it could be stored for decades to centuries. The export efficiency was comparable to other oceanic regions (Berelson, 2001). This conclusion is not consistent with the traditional view of polar marine ecosystems with short food chains dominated by diatoms and high export efficiency. In a recent analysis of high latitude Arctic polynyas and seas, export efficiencies were also consistently lower than expected, even when productivity was high (Tremblay et al., 2012). Lower efficiencies were at least partially explained by blooms that were not dominated by diatoms (Henson et al., 2012), as was the case for the central ASP during our cruise.

Questions for future research

The Amundsen Sea Polynya is remote, difficult to access, and thus rarely visited. Yet, it is important to continue to investigate in future expeditions for several reasons. The ASP is located in one of the most rapidly and profoundly changing regions on the planet. We need to understand the processes underlying its high productivity and role in carbon cycling and storage. We lack even a qualitative understanding of how the ASP ecosystem will respond to continued sea ice loss and the accelerated erosion and possible collapse of the West Antarctic ice shelves. The biogeochemical and ecological implications of changes in the physical environment and primary production system are even less well understood. Among the unanswered questions remaining from our study are the following. Why did the phytoplankton blooms in 2010–2012 terminate before the ice advance? What initiates the particle export events? Is the high flux in winter derived from resuspension and lateral transport of previously deposited production? Why is the flux attenuation pronounced ($b > 1$) compared to some other ocean locations ($b = 0.6–1.2$)? Does dominance by *Phaeocystis* contribute to low export efficiency? Finally, we need better measurements of the current field in the vicinity of the sediment traps and more comprehensive measurements of particle decomposition rates to understand the true relationship between net community production in the surface layer, the export flux and the particle flux captured in sediment traps. Answering these questions requires not only ship occupations of the ASP, but also development of new autonomous sensing systems for expanded year-round observations in the areas with the greatest ice cover and prolonged winter.

References

- Alderkamp A-C, van Dijken GL, Lowry KE, Connelly TL, Lagerström M, et al. 2015. Fe availability drives phytoplankton photosynthesis rates in the Amundsen Sea Polynya, Antarctica. *Elem Sci Anth*: in press.
- Amiel D, Cochran J. 2008. Terrestrial and marine POC fluxes derived from ^{234}Th distributions and $\delta^{13}\text{C}$ measurements on the Mackenzie Shelf. *J Geophys Res-Oceans* **113**: C03S06.
- Amiel D, Cochran J, Hirschberg D. 2002. $^{234}\text{Th}/^{238}\text{U}$ disequilibrium as an indicator of the seasonal export flux of particulate organic carbon in the North Water. *Deep-Sea Res Pt II* **49**: 5191–5209.
- Anadon R, Estrada M. 2002. The FRUELA cruises: A carbon flux study in productive areas of the Antarctic Peninsula (December 1995–February 1996). *Deep-Sea Res Pt II* **49**: 567–583.
- Armstrong RA, Lee C, Hedges JI, Honjo S, Wakeham SG. 2001. A new, mechanistic model for organic carbon fluxes in the ocean based on the quantitative association of POC with ballast minerals. *Deep-Sea Res Pt II* **49**: 219–236.
- Arrigo KR, Brown ZW, Mills MM. 2014. Sea ice algal biomass and physiology in the Amundsen Sea, Antarctica. *Elem Sci Anth* **2**: 000028.
- Arrigo KR, Lowry KE, van Dijken GL. 2012. Annual changes in sea ice and phytoplankton in polynyas of the Amundsen Sea, Antarctica. *Deep-Sea Res Pt II* **71–76**: 5–15.
- Arrigo KR, van Dijken GL. 2003. Phytoplankton dynamics within 37 Antarctic coastal polynya systems. *J Geophys Res* **108**: 3271–3218.
- Banse K. 1990. New views on the degradation and disposition of organic particles as collected by sediment traps in the open sea. *Deep-Sea Res Part A* **37**: 1177–1195.
- Berelson WM. 2001. The flux of particulate organic carbon into the ocean interior: A comparison of four U.S. JGOFS regional studies. *Oceanography* **14**: 59–67.
- Buesseler KO. 1991. Do upper-ocean sediment traps provide an accurate record of particle flux? *Nature* **353**: 420–423.
- Buesseler KO. 1998. The decoupling of production and particulate export in the surface ocean. *Global Biogeochem Cy* **12**: 297–310.
- Buesseler KO, Antia AN, Chen M, Fowler SW, Gardner WD, et al. 2007a. An assessment of the use of sediment traps for estimating upper ocean particle fluxes. *J Mar Res* **65**: 345–416.
- Buesseler KO, Lamborg CH, Boyd PW, Lam PJ, Trull TW, et al. 2007b. Revisiting carbon flux through the ocean's twilight zone. *Science* **316**: 567–570.
- Buesseler KO, McDonnell AMP, Schofield OME, Steinberg DK, Ducklow HW. 2010. High particle export over the continental shelf of the west Antarctic Peninsula. *Geophys Res Lett* **37**: 1–5.
- Butman CA, Grant WD, Stolzenbach KD. 1986. Predictions of sediment trap biases in turbulent flows: A theoretical analysis based on observations from the literature. *J Mar Res* **44**: 601–644.
- Carlson CA, Ducklow HW, Michaels AF. 1994. Annual flux of dissolved organic carbon from the euphotic zone in the northwestern Sargasso Sea. *Nature* **371**: 405–408.
- Chapin III FS, Berman M, Callaghan TV, Convey P, Crepin A-S, et al. 2005. Polar Systems, in Hassan R, Scholes R, Ash N, eds., *Ecosystems and Human Well-being: Current State and Trends*. Washington, DC: Island Press: pp. 717–743.
- Church MJ, Lomas MW, Muller-Karger F. 2013. Sea change: Charting the course for biogeochemical ocean time-series research in a new millennium. *Deep-Sea Res Pt II* **93**: 2–15.
- Cochran JK, Buesseler KO, Bacon MP, Wang HW, Hirschberg DJ, et al. 2000. Short-lived thorium isotopes (^{234}Th , ^{228}Th) as indicators of POC export and particle cycling in the Ross Sea, Southern Ocean. *Deep-Sea Res Pt II* **47**: 3451–3490.
- Collier R, Dymond J, Honjo S, Manganini S, Francois R, et al. 2000. The vertical flux of biogenic and lithogenic material in the Ross Sea: moored sediment trap observations 1996–1998. *Deep-Sea Res Pt II* **47**: 3491–3520.
- Ducklow HW. 1995. Ocean biogeochemical fluxes: New production and export of organic matter from the upper ocean. Reviews of Geophysics. Supplement. (US National Report to IUGG, Contributions in Ocean Sciences). pps. 1271–1276.
- Ducklow HW. 2008. Long-term studies of the marine ecosystem along the west Antarctic Peninsula. *Deep-Sea Res Pt II* **55**: 1945–1948.

- Ducklow HW, Baker K, Martinson DG, Quetin LB, Ross RM, et al. 2007. Marine ecosystems: The West Antarctic Peninsula. *Philos T Roy Soc B* 362: 67–94.
- Ducklow HW, Dickson ML, Kirchner DL, Steward G, Orchard J, et al. 2000. Constraining bacterial production, conversion efficiency and respiration in the Ross Sea, Antarctica, January–February, 1997. *Deep-Sea Res Pt II* 47: 3227–3247.
- Ducklow HW, Doney SC. 2013. What is the metabolic state of the oligotrophic ocean? A debate. *Ann Rev Mar Sci* 5: 525–533.
- Ducklow HW, Erickson M, Kelly J, Smith RC, Stammerjohn SE, et al. 2008. Particle export from the upper ocean over the continental shelf of the west Antarctic Peninsula: A long-term record, 1992–2006. *Deep-Sea Res Pt II* 55: 2118–2131.
- Ducklow HW, Yager PL. 2007. Pelagic bacterial processes in polynyas, in Smith Jr WO, Barber DG, eds., *Polynyas: Windows into Polar Oceans*. New York: Elsevier/CRC: 323–362.
- Fischer G. 1991. Stable carbon isotope ratios of plankton carbon and sinking organic matter from the Atlantic sector of the Southern Ocean. *Mar Chem* 35: 581–596.
- Fischer G, Fuetterer D, Gersonde R, Honjo S, Ostermann DR, et al. 1988. Seasonal variability of particle flux in the Weddell Sea and its relation to ice cover. *Nature* 335: 426–428.
- Fischer G, Gersonde R, Wefer G. 2002. Organic carbon, biogenic silica and diatom fluxes in the marginal winter sea-ice zone and in the Polar Front Region: interannual variations and differences in composition. *Deep-Sea Res Pt II* 49: 1721–1745.
- Forest A, Tremblay J-É, Gratton Y, Martin J, Gagnon J, et al. 2011. Biogenic carbon flows through the planktonic food web of the Amundsen Gulf (Arctic Ocean): A synthesis of field measurements and inverse modeling analyses. *Prog Oceanogr* 91: 410–436.
- Francois R, Honjo S, Krishfield R, Manganini S. 2002. Factors controlling the flux of organic carbon to the bathypelagic zone of the ocean. *Global Biogeochem Cy* 16: 34–41.
- Fransson A, Chierici M, Yager PL, Smith Jr WO. 2011. Antarctic sea ice carbon dioxide system and controls. *J Geophys Res* 116: doi: 10.1029/2010JC006844.
- Gardner WD. 1980. Sediment trap dynamics and calibration: Laboratory evaluation. *J Mar Res* 38: 17–39.
- Giering SLC, Sanders R, Lampitt RS, Anderson TR, Tamburini C, et al. 2014. Reconciliation of the carbon budget in the ocean's twilight zone. *Nature* 507: 480–483.
- Gleiber MR, Steinberg DK, Ducklow HW. 2012. Time series of vertical flux of zooplankton fecal pellets on the continental shelf of the western Antarctic Peninsula. *Mar Ecol-Prog Ser* 471: 23–36.
- Gust G, Byrne RH, Bernstein RE, Betzer PR, Bowles W. 1992. Particle fluxes and moving fluids: Experience from synchronous trap collection in the Sargasso Sea. *Deep-Sea Res Part A* 39: 1071–1083.
- Ha H, Wählin A, Kim T, Lee S, Lee J, et al. 2014. Circulation and modification of warm deep water on the central Amundsen Shelf. *J Phys Oceanogr* 44: 1493–1501.
- Hansell DA. 2002. DOC in the global ocean carbon cycle, in Hansell DA, Carlson CA, eds., *Biogeochemistry of Marine Dissolved Organic Matter*. San Diego: Academic Press: 685–715.
- Hansell DA, Carlson CA. 1998. Net community production of dissolved organic carbon. *Global Biogeochem Cy* 12: 443–453.
- Henson SA, Sanders R, Madsen E. 2012. Global patterns in efficiency of particulate organic carbon flux and transfer to the deep ocean. *Global Biogeochem Cy* 26: GB1028. doi:10.1029/2011GB004099.
- Honjo S, Krishfield RA, Eglinton TI, Manganini SJ, Kemp JN, et al. 2010. Biological pump processes in the cryopelagic and hemipelagic Arctic Ocean: Canada Basin and Chukchi Rise. *Prog Oceanogr* 85: 137–170.
- Honjo S, Manganini SJ, Krishfield RA, Francois R. 2008. Particulate organic carbon fluxes to the ocean interior and factors controlling the biological pump: A synthesis of global sediment trap programs since 1983. *Prog Oceanogr* 76: 217–285.
- Ikeda T, Mitchell AW. 1982. Oxygen uptake, ammonia excretion and phosphate excretion by krill and other Antarctic zooplankton in relation to their body size and chemical composition. *Mar Biol* 71: 283–298.
- Kellogg CTE, Carpenter SD, Renfro AA, Sallon A, Michel C, et al. 2011. Evidence for microbial attenuation of particle flux in the Amundsen Gulf and Beaufort Sea: elevated hydrolytic enzyme activity on sinking aggregates. *Polar Biol* 34(12): 2007–2023. doi:10.1007/s00300-011-1015-0.
- Kellogg CTE, Deming JW. 2014. Particle-associated extracellular enzyme activity and bacterial community composition across the Canadian Arctic. *FEMS Microbiol Ecol* 89: 360–375.
- Kim M, Hwang J, Kim HJ, Kim D, Ducklow HW, et al. 2014. Sinking particle flux in the sea ice zone of the Amundsen shelf, Antarctica. *Deep-Sea Res Pt II*: submitted.
- Knap A, Michaels A, Close A, Ducklow H, Dickson A. 1996. Protocols for the Joint Global Ocean Flux Study (JGOFS) core measurements. JGOFS Report No. 19, vi+170 pp. Reprint of the IOC Manuals and Guides No. 29, UNESCO 1994.
- Laws EA, Falkowski PG, Smith Jr WO, Ducklow HW, McCarthy JJ. 2000. Temperature effects on export production in the open ocean. *Global Biogeochem Cy* 14: 1231–1246.
- Lee SH, Kim BK, Yun MS, Joo H, Yang EJ, et al. 2012. Spatial distribution of phytoplankton productivity in the Amundsen Sea, Antarctica. *Polar Biol* 35: 1721–1733.
- Leventer A, Dunbar RB. 1996. Factors influencing the distribution of diatoms and other algae in the Ross Sea. *J Geophys Res* 101: 18489–18500.
- López-Urrutia Á, Martin ES, Harris RP, Irigoien X. 2006. Scaling the metabolic balance of the oceans. *P Natl Acad Sci* 103: 8739–8744.
- Marsay CM, Sanders RJ, Henson SA, Pabortsava K, Achterberg EP, et al. 2015. Attenuation of sinking particulate organic carbon flux through the mesopelagic ocean. *P Natl Acad Sci* 112: 1089–1094.
- Martin JH, Knauer GA, Karl DM, Broenkow WW. 1987. VERTEX: Carbon cycling in the Northeast Pacific. *Deep-Sea Res Part A* 34: 267–285.
- McConnaughey T, McRoy CP. 1979. Foodweb structure and the fractionation of carbon isotopes in the Bering Sea. *Mar Biol* 53: 257–262.
- Meredith MP, King JC. 2005. Rapid climate change in the ocean west of the Antarctic Peninsula during the second half of the 20th century. *Geophys Res Lett* 32: doi:10.1029/2005GL024042.
- Mu L, Stammerjohn SE, Lowry KE, Yager PL. 2014. Spatial variability of surface $p\text{CO}_2$ and air-sea CO_2 flux in the Amundsen Sea Polynya, Antarctica. *Elem Sci Anth* 2: 000036.

Antarctic particle flux

- Najjar RG, Sarmiento JL, Toggweiler JR. 1992. Downward transport and fate of organic matter in the ocean: Simulations with a general circulation model. *Global Biogeochem Cy* 6: 45–76.
- O'Reilly JE, Maritorena S, O'Brien MC, Siegel DA, Toole D, et al. 2000. SeaWiFS post launch calibration and validation analyses, Part 3. NASA Technical Memo 2000–206892, Volume 11. Washington DC: NASA. 49pp.
- Piñones A, Hofmann EE, Dinniman MS, Klinck JM. 2011. Lagrangian simulation of transport pathways and residence times along the western Antarctic Peninsula. *Deep-Sea Res Pt II* 58: 1524–1539.
- Quay PD, Peacock C, Björkman K, Karl DM. 2010. Measuring primary production rates in the ocean: Enigmatic results between incubation and non-incubation methods at Station ALOHA. *Global Biogeochem Cy* 24: GB3014.
- Randall-Goodwin E, Meredith MP, Sherrell RM, Jenkins A, Yuan X, et al. 2015. Water mass structure and freshwater distributions in the Amundsen Sea Polynya, Antarctica. *Elem Sci Anth*: in press.
- Rau GH, Takahashi T, Des Marais DJ. 1989. Latitudinal variations in plankton $\delta^{13}\text{C}$ implications for CO_2 and productivity in past oceans. *Nature* 341: 516–518.
- Sailey SF, Ducklow HW, Moeller HV, Fraser WR, Schofield OM, et al. 2013. Carbon fluxes and pelagic ecosystem dynamics near two western Antarctic Peninsula Adélie penguin colonies: an inverse model approach. *Mar Ecol-Prog Ser* 492: 254–272.
- Sampei M, Sasaki H, Forest A, Fortier L. 2012. A substantial export flux of particulate organic carbon linked to sinking dead copepods during winter 2007–2008 in the Amundsen Gulf (southeastern Beaufort Sea, Arctic Ocean). *Limnol Oceanogr* 57: 90–96.
- Sampei M, Sasaki H, Makabe R, Forest A, Hattori H, et al. 2011. Production and retention of biogenic matter in the southeast Beaufort Sea during 2003–2004: insights from annual vertical particle fluxes of organic carbon and biogenic silica. *Polar Biol* 34: 501–511.
- Savidge DK, Amft JA. 2009. Circulation on the West Antarctic Peninsula derived from 6 years of shipboard ADCP transects. *Deep-Sea Res Pt I* 56: 1633–1655.
- Siegel DA, Deuser WG. 1997. Trajectories of sinking particles in the Sargasso Sea: modeling of statistical funnels above deep-ocean sediment traps. *Deep-Sea Res Pt I* 44: 1519–1541.
- Smith Jr WO, Anderson RF, Keith Moore J, Codispoti LA, Morrison JM. 2000. The US Southern Ocean Joint Global Ocean Flux Study: an introduction to AESOPS. *Deep-Sea Res Pt II* 47: 3073–3093.
- Smith Jr WO, Gordon LL. 1997. Hyperproductivity of the Ross Sea (Antarctica) polynya during austral spring. *Geophys Res Lett* 24: 233–236.
- Stammerjohn S, Massom RA, Rind D, Martinson D. 2012. Regions of rapid sea ice change: An inter-hemispheric seasonal comparison. *Geophys Res Lett* 39: doi:10.1029/2012GL050874.
- Stammerjohn SE, Martinson DG, Smith RC, Iannuzzi SA. 2008. Sea ice in the western Antarctic Peninsula region: Spatio-temporal variability from ecological and climate change perspectives. *Deep-Sea Res Pt II* 55: 2041–2058.
- Steinberg DK, Martinson DG, Costa DP. 2012. Two decades of pelagic ecology of the Western Antarctic Peninsula. *Oceanography* 25: 56–67.
- Takahashi T, Sutherland SC, Wanninkhof R, Sweeney C, Feely RA, et al. 2009. Climatological mean and decadal change in surface ocean pCO_2 , and net sea-air CO_2 flux over the global oceans. *Deep-Sea Res Pt II* 56: 554–577.
- Tremblay J-E, Dominique R, Varela DE, Lovejoy C, Darnis G, et al. 2012. Current state and trends in Canadian Arctic marine ecosystems: I. Primary production. *Clim Change* 115: doi: 10.1007/s10584-012-0496-3.
- Weston K, Jickells TD, Carson DS, Clarke A, Meredith MP, et al. 2013. Primary production export flux in Marguerite Bay (Antarctic Peninsula): Linking upper water-column production to sediment trap flux. *Deep-Sea Res Pt I* 75: 52–66.
- Williams CM, Dupont AM, Loevenich J, Post AF, Dinasquet J, et al. 2015. Pelagic microbial heterotrophy in response to a highly productive bloom of *Phaeocystis antarctica* in the Amundsen Sea Polynya, Antarctica. *Elem Sci Anth*: in press.
- Wilson SE, Swaethorp R, Kjellerup S, Wolvertson MA, Ducklow HW, et al. 2015. Meso- and macro-zooplankton community structure of the Amundsen Sea Polynya, Antarctica (Summer 2010–2011). *Elem Sci Anth* 3: 000033.
- Yager P, Sherrell R, Alderkamp A, Ingall E, Ducklow H. 2014. Net Community Production and Export in the Amundsen Sea Polynya (Western Antarctica); with Comparisons to Arctic Polynyas and a Link to Climate Sensitivity. 17th Ocean Sciences Meeting, Honolulu, HI. 26 February 2014.
- Yager PL, Sherrell RM, Stammerjohn SE, Alderkamp A-C, Schofield O, et al. 2012. ASPIRE: The Amundsen Sea Polynya International Research Expedition. *Oceanography* 25: 40–53.

Contributions

- Contributed to conception and design: HWD, ME, SEW, PLY
- Contributed to acquisition of data: HWD, ME, AFP, SHL, KEL, RMS, SES, SEW
- Contributed to analysis and interpretation of data: HWD, RMS, SEW, PLY
- Drafted and/or revised the article: HWD
- Approved the submitted version for publication: HWD, SEW, AFP, SES, ME, SHL, KEL, RMS, PLY.

Acknowledgments

We acknowledge the following individuals and organizations for assistance in our study: the captains, officers and crews of RVIB NB Palmer (NBP10–05) and RVIB Araon; the Korean Polar Research Institute (KOPRI); P. Abrahamson (UK-BAS) and R. Guerrero for able support deploying (NBP) and recovering (KOPRI, Araon) our mooring; Raytheon Polar Services for science support during the entire ASPIRE project; and M. Conte and J.C. Weber (MBL Ecosystems Center) for help with sample analysis. A. Bausch and J-E. Tesdal (LDEO) recovered the WAP Chl data. B. Hönisch (LDEO) kindly loaned her dissecting microscope and digital camera for Figure 7. Thanks also to all our colleagues in ASPIRE for fruitful and stimulating discussion and support throughout the project.

Antarctic particle flux

Funding information

The ASPIRE Project was supported by the Antarctic Organisms and Ecosystems Program at the US NSF Office of Polar Programs, award ANT 0839012 to HWD, ANT-0839069 to PY, ANT-0838995 to RMS, ANT 1142095 to AFP, ANT-0838975 to SS, and ANT-0944727 to K Arrigo for support of KEL. Trap recovery by RVIB Araon was supported by KOPRI Award PP12020 to S. H. Lee. WAP research was supported by NSF-ANT 0823101 and 1440435.

Competing interests

None of the authors declares a competing interest for the work reported in this publication.

Data accessibility statement

ASP sediment trap data are available at the BCO-DMO website (BCO-DMO ASPIRE site, <http://www.bco-dmo.org/project/2132>). Palmer LTER data are available at: ([http://oceaninformatics.ucsd.edu/datazoo/data/pallter/datasets; Dataset number 26, "Offshore sediment trap fluxes"](http://oceaninformatics.ucsd.edu/datazoo/data/pallter/datasets;Dataset%20number%2026,%20%22Offshore%20sediment%20trap%20fluxes%22)).

Copyright

© 2015 Ducklow et al. This is an open-access article distributed under the terms of the Creative Commons Attribution License, which permits unrestricted use, distribution, and reproduction in any medium, provided the original author and source are credited.